American Journal of Analytical Chemistry, 2025, 16(3), 23-41
https://www.scirp.org/journal/ajac
ISSN Online: 2156-8278
ISSN Print: 2156-8251

Winterizing and Use of a Solar Box Cooker on the Island of Crete, Greece

James F. Lalor[1], Victor J. Law[2*], Denis P. Dowling[2]

[1]School of Mechanical Engineering, Technical University Dublin, Dublin, Ireland
[2]School of Mechanical and Materials Engineering, University College Dublin, Dublin, Ireland
Email: *viclaw66@gmail.com

How to cite this paper: Lalor, J.F., Law, V.J. and Dowling, D.P. (2025) Winterizing and Use of a Solar Box Cooker on the Island of Crete, Greece. *American Journal of Analytical Chemistry*, **16**, 23-41.
https://doi.org/10.4236/ajac.2025.163003

Received: March 1, 2025
Accepted: March 28, 2025
Published: March 31, 2025

Abstract

This study investigated the performance of a winterized inclined window solar box cooker (SBC) designed for cooking of foodstuff during the 2 months on either side of the winter solstice (21st December, northern hemisphere) in the White mountains of Crete Greece (35.31˚N, 24.31˚E, altitude of 150 m). In order to assess the performance of the SBC, the energy required for cooking of whole liquid eggs is calculated and compared with the performance of non-winterized SBC at the same location (27th July 2024). For both SBC measurements, the energy required for cooking of whole liquid eggs without water was between 0.53 ± 0.06 $kJ·g^{-1}$ for a solar irradiance between 873 and 1004 $W·m^{-2}$. Although the winterized SBC can only work for a few consecutive sunshine days in February, it has the potential to operate between violent storms that bring down overhead electrical lines and disrupt road transport links. In this short, but challenging, period people still need to eat and have access to clean drinking water. Hence a ready-to-use winterized SBC enables remote isolated communities to become self-sufficient in the short-term using free sunshine energy.

Keywords

Solar Box Cooker, Solar Radiation, Winter Storms, Food Cooking Metrics

1. Introduction

The abundance of freely available solar energy throughout the tropical and temperate climate regions allows remote and off-grid communities to use solar stoves to pasteurize water and cook their daily meals, Kerr (1991) [1]. While solar stoves that include panel, box, and vacuum tube designs, do not fix environmental degradation problems, or a family's basic necessities of shelter, clean water, and medical care in an emergency situation: it can provide an alternative free energy source to centralized electrical supply and fossil fuel resources to cook foodstuff in sunshine hours. The low cost and easy-use of these solar stoves mean that kitchen-sets containing the essentials for solar cooking are supplied to people within humanitarian camps that are setup following natural disasters, Regattieri *et al.* (2016) [2]. In the Mediterranean basin region the solar box cooker (SBC), these stoves are constructed as a plywood cuboid-like structure topped with an inclined transparent window, Law *et al.* (2024) [3]. Where the role of the window is to allow solar short-wavelength radiation in and trap longer-wavelength radiation from heated objects within the box. This greenhouse heating effect produces medium-low temperatures sufficient for the pasteurization of naturally contaminated water and cooking foodstuff over a period of a few hours with the loss of vitamins and essential nutrients, which would be lost when frying, or roasting, temperatures. At least one, or up to six external reflection surfaces are employed for directing additional sunlight into the box. In the Eastern Mediterranean temperate region, the summer solstice (21st June, in the northern hemisphere) rule of thumb is that SBC's window is orientated to the south with an inclined tilt angle (θ) that approximates the local latitude (ϕ) minus an annual weighted angle (ϕ_w) of 3 - 4 degrees [3]-[7]. This configuration maximises solar capture around solar noon when most cooking occurs. The tilt angle also applies to Mediterranean fixed photovoltaic solar panels to maximize energy generation over the entire year (Darhmaoui and Lahjouji (2013) [8], Kambezidis and Psiloglou (2021) [9], and Abu-Naser (2024) [10]). This rule of thumb is mathematically expressed in Equation (1).

$$\theta = \varnothing - \varnothing_w \tag{1}$$

On the island of Crete that has nominal latitude of 35 degrees, a south-orientated SBC therefore has an inclined window θ of approximately 31 degrees. To maintain efficient solar cooking at the winter solstice (21st December, in the northern hemisphere) it is preferable to increase the inclined window θ to 44 to 46 degrees **Figure 1**. In this figure, the difference between the two solstice angles reflects the Earth's Axial tilt around its orbital axis.

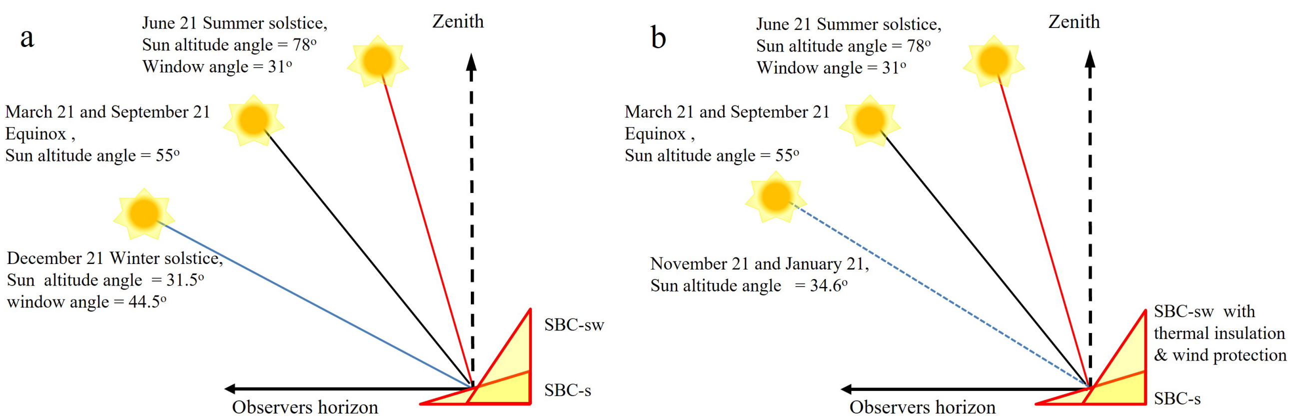

Figure 1. 2D view of inclined window SBC on the island of Crete (ϕ~35˚) summer solstice requirements (a). Winter solstice with additional environmental protection requirements (b).

Away from the Mediterranean, for example, Mexico (18.50˚N), Jaramillo *et al.* (2007) [11] added an additional internal surface to the SBC structure to create a north-south orientated irregular pentagon cross-section that allows two pentagon sides to be used as a base. This dual "optogeometrical" design (here termed "dual aspect inclined window") enables SBC positioned away from the equator to heat water and cook foodstuff efficiently in different seasons: one orientated for the summer months and one originated for the winter months. Chatelain *et al.* (2009) [12] also used a dual aspect inclined design for Lausanne Switzerland (46.51˚N, 6.63˚E) with the potential of 155 to 240 number of cooking days depending on the canton location. In the city of Sana'a, Yemen (15.4˚N, 44.2˚E) Al-Nehari *et al.* (2021) [13] constructed a variable inclined window SBC by using an external jack to tilt the SBC window for optimum solar cooking. In all cases, to maintain efficient solar heating within the SBC is aligned to the Sun's azimuth and altitude angle within the sky. For the manual azimuth alignment, the SBC is rotated (typically every 15 to 20 minutes) towards the Sun throughout the day.

Returning to the island of Crete in Eastern Mediterranean where a south orientated dual aspect window SBC is used, it is necessary to understand the combined processes of the Sun's solar beam interaction with the SBC and the local seasonal environmental conditions that impact on the SBC cooking performance, in particular the extreme winter weather events (Greenberg *et al.* (2007) [14]). In the western regions of Crete, autumn generally begins in October when natural climate variations drive cool winds from the north to mix with the warm sea surface surrounding the island to produce a moist laden cloud in the Lefka Ori **Figure 2 (a)** with the heights peaks named Mt. Pachnes, 2453 m) and Mt. Psiloritis 2456 m further to the east. From November the winds become colder driving-down day and night temperatures that increase cloud cover and further precipitation in the

Figure 2. Looking south form Kalyves to the Lefka Ori; picture taken on 24.1.2025 (a). The collapsed stone bridge over the Ketritis River south of Chania, Crete, Greece (b); picture taken on 24.8.2019.

mountains. During this seasonal period quasi-stationary high pressure Omega blocking systems over mainland Greece (150 km to the north of Crete), with lows to the southeast and southwest, (Detring *et al.* (2021) [15]) produce fair weather periods that help the Cretan oil harvest season. However, when the blocking system breaks down in late November to early December the inrush of low-pressure systems leads to heavy rainfall with low temperatures. For example, in February 2019 two storms (Chioni and Oeanis) caused four deaths, and brought down overhead electrical power lines, crippled road infrastructure due to the destruction of the stone road bridge spanning the Keritis river, south of Chania **Figure 2(b)**, plus widespread landsides and flooding: leaving rural communities in western Crete isolated for multiple days (Lagouvardos *et al.* (2020) [16]).

Solar cooking in these unfavourable weather conditions and short daylight hours (approximately nine hours, forty-seven minutes on the 21st of December) is a challenge. In addition in mountainous valleys morning and afternoon shadowing further reduces day light hours to six to seven hours per day **Figure 3**. Despite these winter conditions the potential to solar cook in periodic fair weather periods remains (Chatelain [12] and Soro *et al.* (2007) [17]). Furthermore, a number of solar cooker web sites [18] [19] discuss the inclusion of a ready-to-use solar stove in a family's emergency/disaster preparedness plans where under these temporary weather conditions the immediate utility value of the solar stove is invaluable as it reduces the reliance on relief supplies that may take many days to arrive.

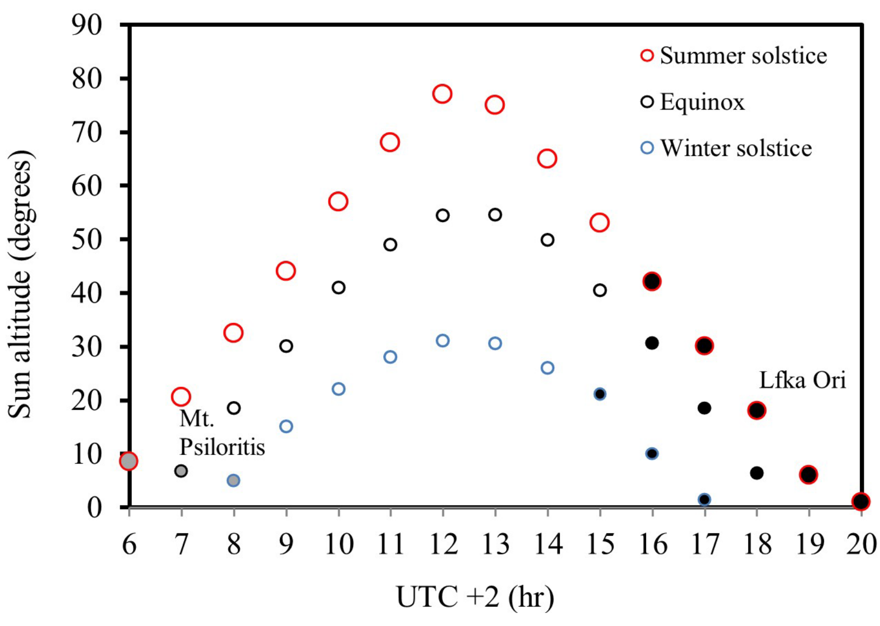

Figure 3. Solar graph depicting sun altitude and daylight duration for summer and winter solstice and Equinox for village location (35.31˚N, 24.31˚E, altitude of 150 m). The light gray filled markers represent Sunrays blocked by Mt. Psiloritis and the dark black filled markers represent sunrays blocked by the Lefka Ori.

The aim of this work is twofold. First, to modify and develop the inclined window SBC as described [3] into a dual aspect inclined window SBC for all-year-round cooking of foodstuff on the island of Crete. The second aim is to establish a SBC pre-charging (preheating) for the months of January and February when the night-time temperatures drop below < 8˚C. Henceforth the winterized SBC is termed SBC-sw (sw stands for summer and winter use), and the original design is termed SBC-s (where s stands for summer use). As with unfavourable weather conditions, the SBC-sw is expected to heat water and cook foodstuff slower than under full sunshine conditions but still reach temperatures sufficient for pasteurization/purification of water ([1] [2] and Ciochetti and Metcalf (1984) [20]).

Given that the SBC has successfully cooked rice, pasta and eggs-without water where the latter was compared to solar-cooked eggs (cooked with and without water) reported in eleven scientific journals [3], the foodstuff of choice is fresh whole eggs solar cooked without water. The egg size ranges from 53 to 65 grams. This foodstuff choice is for the four following reasons:

1) It removes the need to use scarce water resources in drought stresses regions, or when the water source becomes polluted after violent storms.

2) The removal of water from the cooking process eliminates a major energy component in the study thereby enabling the energy imparted in the eggs to be isolated.

3) The eggs are solar cooked without water to a hard boiled state. In this process the whole liquid egg (yolk and albumen) undergoes an irreversible chemical and physical change without the loss of the nutritional integrity of the egg. Typically, the inner yellow yolk begins to denature at 62˚C and solidifies at around 70˚C and the protective outer translucent albumen denatures in the range of 60˚C to 84˚C [21] [22].

4) The SBC-sw solar cooked egg study reported here allows a direct comparison with previous s solar cooked egg study performed in the SBC-s at the same location.

To support this comparison, no reversible phase change material (PCM) [7] [23]-[30] employed, nor is the SBC external reflector surface changed from aluminum foil to a glass mirror.

2. SBC-sw Design

Constructing a SBC to operate in the winter months where the number of available sunshine days is greatly reduced, the build cost is a major economic factor ([5], Bhaumik *et al.* (2018) [25], and Poonia and Singh (2024) [30]. For this reason, local carpentry skills and available sourced materials is used, with a focus on retaining the SBC portability by minimising additional material and weight. Finally, the local carpentry workshop constructs the SBC. **Figure 4** shows photograph of the completed SBC-sw, exploded component view of the SBC-sw, and 150 mm truncated wedge fixed to the metal tripod on which the SBC seats and rotates. Repurposing of cardboard based material (CBM) [2] for the main structure of the

SBC-sw is unsuitable as the amount of rainfall in the winter months of Crete destroys the structure within one winter season. Durable machined materials (plywood) and glass is the structural material used as it extends the SBC lifespan over a number of winter seasons. This choice does not extend to the outer cover of SBC that adds thermal insulation and wind protection. The lifespan of the CBM cover is one winter season and at the end of the season the cover is recycled into garden waste.

The SBC-sw is modified from the SBC-w by reversible changes that come under the following modification categories:

1) Inclined window modification

a) In the winter months low incline solar angles have a significant role in the solar cooking process. Therefore to improve solar access at these angles a section (length = 280 mm, width = 20 mm, depth = 20 cm; with a virtual incident collection area (a_i) = 0.0044 m^{-2}) is removed from the SBC top two south-orientated front panels (**Table 1**, component 1 and 2, **Figure 4(a)**). This modification adds to the SBC virtual incident collection area (A_i), defined by the diagonal distance between the external reflector panel top edge and the front edge of the SBC multiplied by the SBC width. **Figure 4(a)** denotes a_i and A_i with yellow dashed lines.

b) To increase the inclined window angle to 45˚, a 15˚ truncated wedge (L = 320 cm; with a cross-section of 13 cm × 9.5 cm × 7 cm). A volume within the wedge is removed to reduce the wedge weight to 0.974 kg. The wedge was then fixed with a dowel pin to the repurposed metal tripod **Figure 4(c)**.

2) Absorber plate angle modification

To accommodate the new inclined angle, the 2 mm diameter stainless-steel wire frame that supports the absorber plate is adjusted by 15˚. This is achieved by inserting a wooden bracket (**Table 1**, component 16) on the inner south-orientated panel, measuring 280 mm in length, 10 mm in width, and 20 mm depth, with 15˚ inclined top, depth = 2 cm. The metal absorber plate is made from dark enamelled mild steel: 0.08 cm thickness with rolled edge L = 28.5, w = 23, and h = 6 cm and surface area of approximately 0.154 m^2, mass = 0.31 kg, and a surface-area-to-mass ratio of approximately 0.513 $m^2 \cdot kg^{-1}$. However, this modification, combined with the raised internal floor (b) constrains the available internal space for cooking vessel.

3) Insulation modification

a) To improve thermal SBC insulation, a 9 mm thick plywood panel (0.4 kg) lined with aluminium foil sheet is placed on the top of the original bottom surface (**Table 1**, component 15).

b) To insulate from the winter temperatures and winds, repurposed corrugated CBM is adhered to the outside of SBC. The CBM is the material of choice as it is lightweight, and a low cost alternative to plywood and other insulation materials (Čekon *et al.* (2017) [31]). For construction, a 1 cm thick CBM composite layer is formed (depending upon availability two to three sheets are taped together) with one side backed with aluminium foil; with an approximate weight of 0.35 kg).

a

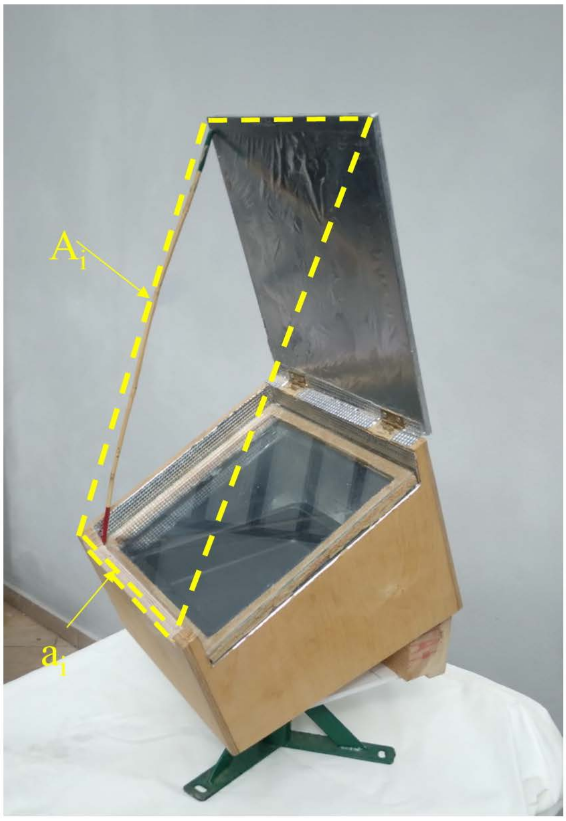

b

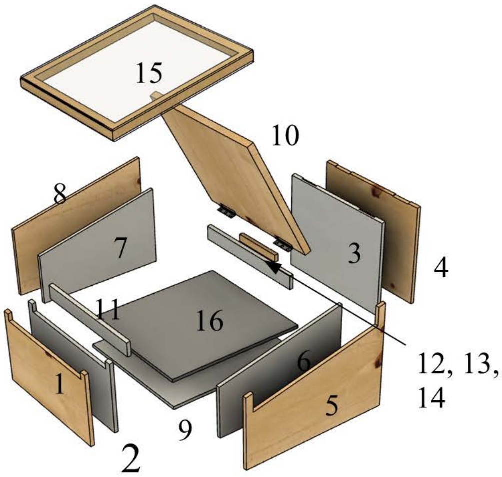

c

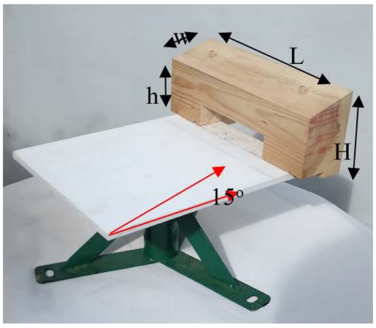

Figure 4. Photograph of complete SBC-sw positioned on the tripod with the 15˚ truncated wedge: the area within the yellow dash line denotes a_i and A_i. For clarity, the wind protection CBM layer is not shown (a). AutoCAD® exploded view of SBC-sw with numerated component parts Table 1 (b). Close-up photograph of metal tripod with truncated 15˚ wedge (c).

Table 1. SBC-sw component list with overall dimensions.

Item	Number	Material	Description	Length (mm)	Width (mm)	Depth (mm)
1*	1	Marine plywood	Front out panel	312	202.25	9
2*	1	Marine plywood	Front inner panel	312	195.5	9
3	1	Marine plywood	Back outer panel	312	288.5	9
4	1	Marine plywood	Back inner panel	312	277.2	9
5	1	Marine plywood	Right side outer panel	360	288.5	9
6	1	Marine plywood	Right side inner panel	324	225	9
7	1	Marine plywood	Left side inner panel with inner reduced height for glass window	324	225	9
8	1	Marine plywood	Left side outer panel	360	288.5	9
9	1	Marine plywood	Bottom panel	342	312	9
10	1	Marine plywood	External reflector panel	371	330	6
11	1	Marine plywood	Front rail	294	40	9
12	1	Marine plywood	Back rail	294	40	9
13	2	Brass	Folding hinge	40	20	6
14	1	Marine plywood	External reflector brace	150	20	9

Continued

15	1	Glass and cork	Double glazed unit	325	310	20
16**	1	Marine plywood	Internal base panel	324	294	9
17**	1	Marine plywood	Internal wire frame support bracket	Typically 2 mm stainless steel wire		
18**	1	Reused CBM	Outside thermal insulation and wind protection	Typically 10 mm thick		

*Modification to existing SC-s. **New component.

Build cost and comparison of SBC-sw

Table 2 provides the original SBC-s build cost (May 2024) and the conversion build cost to the SBC-sw (October 2024) and their respective weight. The costs include the labour and materials from local carpentry workshops, and farm metal workshop. The SBC outer CBM covering is repurposed form local submarket packaging; also the tape bought at the local supermarket. Using this approach the total cost of the original design of 107 Euro to 142 Euro and when adjusted for US-Dollars (exchange rate 1.09) the cost equates to 154.78 US-dollars. In terms of weight (including metal tripod), the SBC-sw additional weight is some 1.75 kg making a total weight of 18 kg.

Table 2. SBC manufacture costs and weight.

Item	Date	Euros	Weight (kg)
SBC-s	May 2024	107	~16.25
Conversion to SBC-sw	October 2024	35	~1.75
Total		142	~18

A comparison of the above costs with other SBC built after 2022 can be found in [3]. For example: Benbaha *et al.* (2023) [5] provide a 2023 guide price of €223 to €335, Kumar *et al.* (2022) [27] provides a cost of €45 to €143; and Kumar *et al.* (2023) [28] provides a price guide of approximately 48 US-Dollars. From these reported SBC construction cost described here is in line with recent reported build costs in both India and Algeria.

3. Experimental

All the SBC-sw heating and cooking experiments are performed at the mountain village location (35.31˚N, 24.31˚E, altitude of 150 m). Coordinated Universal Time plus two hours (UTC +2 hrs) is used throughout the study. The solar irradiance values at the cooking site are obtained from SunCalc open-source software (https://www.suncalc.org) and vary between 1004 and 873 W·m^{-2}. Ambient temperature is measured in the shade using a digital thermometer (temperature range −50˚C to 300˚C, with accuracy of 1˚C at 20˚C). For hygiene purposes two stainless-steel analogue dial temperature probes are used for measuring the SBC absorber plate and the internal temperature of the eggs. The probes have a temperature range of 0 to 120˚C, with accuracy of 1˚C for measuring the absorber plate temperature, and a 0˚C to 100˚C, with accuracy of 1˚C for measuring the eggs. Relative air humidity measurements were not recorded.

Stagnation (loaded) temperature profiles

This assess the effect of cloud cover on temperature profiles with the SBC-sw stagnation (unloaded) measurement are performed and used to inform when solar cooking should be carried out

SBC-sw winter storage

Ensuring minimum environmental degradation, due to morning dew, rain, and wind, the SBC-sw, along with its CBM protective outer layer, it is brought indoors overnight for the months of December, through to February. Under these protective conditions the night-time temperatures are typically 20˚C. On solar cooking days the SBC-sw is taken outside (8.30 to 9.00 a.m.) and repositioned at the cooking site The SBC-sw is then aligned to the Sun with the external reflector angled to maximise sunlight entering the box. In the summer months (March through to November) both SBC are stored at the cooking site under a canvas cover with night-time temperatures are between 12˚C to 22˚C.

SBC-sw preheating

Once the SBC-sw is positioned at the cooking site the SBC-sx external reflector is opened to allow it and the absorber plate to be preheated by the Sun. Manual azimuth solar and solar altitude alignment is performed every 15 to 20 minutes

Solar cooking of eggs-without water

Prior to cooking, the eggs are stored indoors at room temperature (20˚C to 22˚C). The eggs solar cooking process is as follows. The eggs are placed in a cut down cardboard egg box container, which is placed on the preheated (95˚C) absorber plate. [***N.B***. A photograph of this procedure is given in reference [3], Figure 10B). The use of the cardboard egg container is twofold.

1) The cardboard container prevents the eggs from rolling and cracking against each other.

2) The cardboard prevents egg direct contact with the hot absorber plate; otherwise the egg shells begin to burn. At the end of the cooking process the container and egg shells are recycled as garden waste [3].

SBC performance metric

The generally accepted form of the First figure of merit (F_1), Equation (2) ([3], Collares-Pereira (2018) [32] and Folaranmi (2013) [33] is used to define the unloaded sensible temperature measurements of the SBC with an external reflector. In this equation, the absorber plate temperature (T_{abs}; must be above the boiling temperature of water and measured in ˚C), and T_{amb} is the outside ambient temperature. The difference in these two temperature terms is then divided by solar irradiance (H_s; measured in the horizontal plane and expressed in units in $W \cdot m^{-2}$). The advantage of using this equation is that the chosen terms are easy to measure to provide a snap-shot in-time of the balance of heat input to heat loss at the absorber plate. The F_1 metric is useful in comparing the performance of one unloaded solar cooker to another unloaded cooker when the solar irradiances of each measurement are not too dissimilar. The F_1 metric however has their drawback in that many seasonal environmental factors and SBC design features are compressed (or reduced) into three terms and therefore does not capture the difference and nuances between SBC designs and local environmental factors.

$$F_1 = \frac{T_{abs} - T_{amb}}{H_s}, \text{ measured in units of } {}^\circ\text{C m}^2\cdot\text{W}^{-1} \quad (2)$$

A more realistic first figure of merit includes the SBC solar concentration ratio (A_i divided by A_{abs}), where A_{abs} is the absorber plate area as defined by F_1' [5] [32] [33] Equation (3). Given that A_{abs} is directly measured and A_i is determined using both engineering drawings and measurements.

$$F_1' = \frac{A_i}{A_{abs}} \frac{T_{abs} - T_{amb}}{H_s}, \text{ measured in units of } {}^\circ\text{C m}^2\cdot\text{W}^{-1} \quad (3)$$

Given the limitation of the first figure of merit, Equations (1) and (2) are used to evaluate and compare the SBC-sw with its original design (SBC-s) over a seven-month period May to October 2024 at one location, see Section 4.

Estimation of cooking power

The calorimetric open water-dish load method is expressed in Equations (4) and is used to estimate the thermal power needed to heat the eggs-without water [3].

$$P = mC\frac{\Delta T}{\delta t} \quad (4)$$

where P is the applied power (W, or J s^{-1}), m is the mass (g) of material, C is the material heat capacity 4.184 J·g^{-1}·K^{-1} for water, 3.23 J·g^{-1}·K^{-1} for liquid whole egg [34], ΔT is the change in temperature of heated foodstuff (final temperature minus the initial temperature), and δt is the heating time interval (s). Where T varies with t in a dynamic reaction, it is normal to take the tangent of the initial temperature curve ($t = 0$) to obtain P. The process energy budget therefore equates to P multiplied by the solar cooking time measured in seconds. Dividing this value by the mass of material heated (cooked) yields the process energy density, measured in J·g^{-1}.

4. Unloaded SBC-sw Sensible Temperature Tests

The unloaded SBC sensible temperature tests were performed on the following days 5.19.2024, 24.10.2024 and 27.10. 2024, with solar irradiance values of 974, 845, and 960 W·m^{-2}, respectively. Each test started at 8.0 a.m. and finished at 2.30 p.m. UTC +2 hr time with the SBC manually aligned to the Sun's geographic azimuth position every 15 to 20 minutes. At the same time, the external reflector angle is adjusted to direct the solar radiation on to the absorber plate by increasing the bamboo length using the following fix lengths: 46, 51, 53, and 60 cm. Temperature measurements of the cooking vessel and ambient air were also taken every 15 minutes.

Figure 5 shows the result of the three unloaded sensible temperature test as a function of time. Here it is seen the 27.10.2024 data (open squares) produces the highest (105˚C) and most stable ($t = 12$ to 14.5 p.m.) absorber plate temperature.

In addition, the initial temperature slope ($\Delta T/\delta t$) is some 0.03277 ˚C·s^{-1}. A comparison with the other two initial temperature slopes (15.10.2024 and 24.10.2024) shows they have $\Delta T/\delta t$ values of 0.024 and 0.01926, respectively. This information shows how cloud cover would affect solar cooking studies. Using this information, non-cloud-covered mornings were chosen for the solar cooking studies.

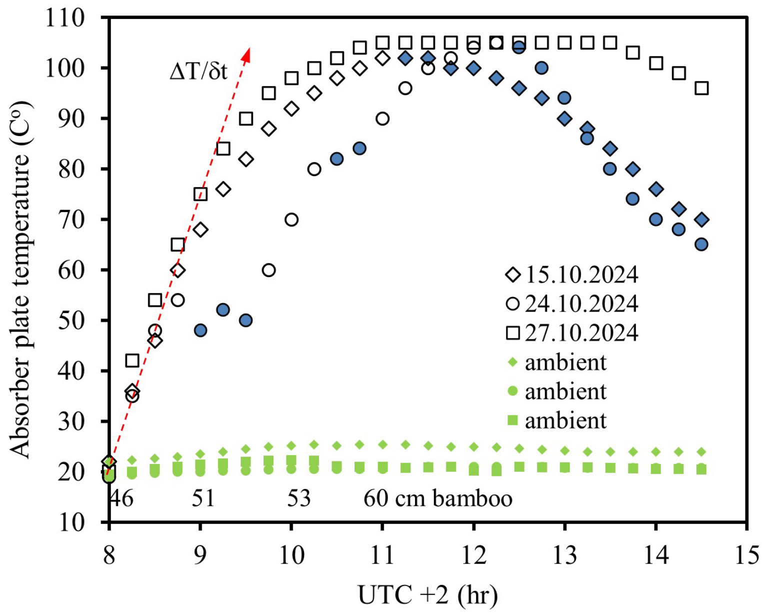

Figure 5. SBC-sw stagnation (unloaded) temperature profiles for bamboo lengths: 46, 51, 53, and 60 cm. Open diamonds, circles and squares represent full sunshine, dark blue filled diamonds, circles and squares represent the Sun obscured by cloud. Small green filed diamonds, circles, and squares represent ambient temperatures. The measurements performed in the mountain village location on 15.10.2024, 24.10.2024, and 27.10.2024.

Table 3. SBC-sw F_1 and F_1' results compiled from **Figure 4** and SunCalc software.

Date	Ambient temperature (˚C)	Absorber Temperature (˚C)	Irradiance (W·m^2)	F_1 (˚C m^2·W^{-1})	A_i (m^2)	A_{abs} (m^2)	F_1' (˚C m^2·W^{-1})
15.10.2024	25	102	974	0.079	0.196	0.152	0.101
24.10.2024	21.1	105	984	0.086	0.196	0.152	0.110
27.10.2024	21	105	960	0.088	0.196	0.152	0.112
Mean	22.36	104	972.66	0.084	0.196	0.152	0.107

Table 3 compiles the F_1 and F_1' data for all three unloaded sensible temperature test along with their mean values. The 27.10.2024 data reveals the highest F_1 and F_1' values 0.088 and 0.012˚C m^2·W^{-1} despite the solar irradiance at the start of the test having the lowest value of 960 W·m^2. For the intermittent cloud days their F_1 and F_1' values are range respectably from 0.79 and 0.086, and 0.101 and 0.11˚C m^2·W^{-1}. These values as previously stated are a snap-shot in-time of the days test and do not reveal the presence of the intermittent cloud formations.

Table 4 presents the mean values of the unloaded SBC-s and unloaded SBC-sw first figure of merit, as defined by Equations (1) and (2). The mean values are computed from three different test days (SBC-s 6th, 7th, and 9th May 2024; and SBC-sw, 15th, 24th, and 27th October 2024). The most striking feature of note is that the F_1 and F_1' values for both SBC are similar. The data reveals the mean October ambient temperature, absorber temperature and solar irradiance are some 5.44˚C, 10˚C, and 39.34 W·m^{-2} lower than the month of May data. For this comparison, the data indicates that introducing the SBC modifications (categories 1 to 4) F_1 and F_1' values are maintained for the period of May to October 2024.

Table 4. Mean SBC F_1 and F_1' data compiled from Table 3 and [3].

SBC (window tilt angle and month)	Ambient temperature (˚C)	Absorber Temperature (˚C)	Solar irradiance (W·m²)	F_1 (˚C m²·W⁻¹)	A_i (m²)	A_{abs} (m²)	F_1' (˚C m²·W⁻¹)
SBC-s (31˚, May)	28.8	114	1012	0.084	0.19	0.152	0.108
SBC-sw (45˚, October)	22.36	104	972.66	0.084	0.196	0.152	0.107
Difference	−5.44	−10	−39.34	0	+0.006	0	−0.001

5. Loaded (Eggs-Without Water) SBC Sensible Heat Test Experiments

This section describes the solar cooking of fresh whole eggs using the SBC-sw during the consecutive months of November 2024 to February 2005. For completeness, a comparison with solar cooking of fresh whole eggs using the SBC-sw is also given.

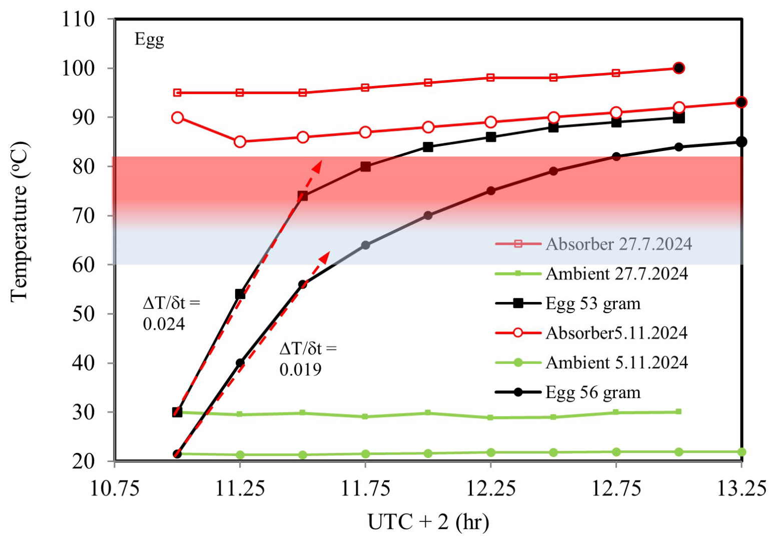

Figure 6. Solar cooking of fresh whole eggs-without water in the SBC-s (27.7.2024) and the SBC-sw (15.11.2024). Red lines represent absorber plate temperature. Black lines represent egg temperature with large black circles denotes the completion of the cooking time. Green markers and lines represent the ambient temperature. The transparent blue to red band represents yolk and albumen denaturation temperature range.

Figure 6 presents data for solar cooking of fresh whole eggs using the SBC-s on 27.17.2024 along with eggs cooked in the SBC-sw on 5.11.2024. In both cases solar preheating began 8.30 to 9.0 a.m. At 11.0 a.m. the double-glazed window is opened, and the container of eggs placed into the SBC followed by the closing of the window. Every 15 minutes throughout the solar cooking stage the SBC was manually aligned to the Sun along with the temperature of one of eggs measured.

Table 5 lists the fresh whole eggs solar cooking metric data for the SBC-sw. For comparison, row two provides the cooking metric data for the SBC-s on 7.7.2024. Weather information is also given for days interspersed between the cooking days. Now follows a description of the cooking metric data.

Column one reveals that as the cooking date progresses from 27.7.2024 to 26.2.2025, the solar irradiance (recorded at 11 a.m.) increases in value from 1004 $W \cdot m^{-2}$ to a minimum of 873 $W \cdot m^{-2}$ on the 18.12.2024 which corresponds to 3 days before the winter solstice, followed by an increase in solar irradiance for the months of January and February 2025. Column two to five provides; the total egg mass cooked, the computed initial 30-minute temperature rate rise, the judged egg cooking time, and the heat capacity of fresh whole eggs (3.3 $J \cdot g^{-1} \cdot K^{-1}$). Columns six to eight lists the resultant computed values of the three eggs; cooking power, cooking energy, and imparted energy density. The values in the last three columns the power and energy values partly follows the solar irradiance values in column one, the reason being that that the total egg mass varies asymmetrically varies from one days study to another. Importantly the egg energy density value (0.580.06 $kJ \cdot g^{-1}$) for the SB-s, and mean value for the SB-sw (0.53 ± 0.06 $kJ \cdot g^{-1}$) are in good agreement.

Table 5. SBC-s and SBC-sw estimated cooking power, cooking energy budget and cooking energy density for liquid whole egg without water. *Hellenic National Metrological Service* (*HNMS*) *warnings*, *and first author's metrological observations*.

SBC-type Date Solar irradiance at 11 a.m.	Total egg mass (g)	$\Delta T/\delta t$	Cooking Time (s)	LWE Cp ($J \cdot g^{-1} \cdot K^{-1}$)	Cooking power ($J \cdot s^{-1}$)	Energy (kJ)	Energy density ($kJ \cdot g^{-1}$)
SBC-s 27.7.2024 1004 $W \cdot m^{-2}$	162	0.0244	7200	3.3	13.068	94.89	0.580
SBC-sw 5.11.2024 935 $W \cdot m^{-2}$	175	0.0194	8100	3.3	11.229	90.95	0.519
18.11.2024	*First snow on Mt. Pachnes* (2453 *m*), *Stratocumulus clouds on Mt. Psiloritis*						
SBC-sw 20.11.2024 910 $W \cdot m^{-2}$	170	0.0233	7200	3.3	13.09	94.24	0.554
30.11.2024	*HNMS storm* "*Bora*" *warning*						
SBC-sw 4.12.2024 879 $W \cdot m^{-2}$	160	0.0194	8100	3.3	11.23	90.95	0.558

Continued

SBC-sw 18.12.2024 873 W·m^{-2}	178	0.0155	9000	3.3	9.14	82.22	0.462
21-26.12.2024	*Winter solstice; rain in the village, snow on Mt. Psiloritis and Likia Ori*						
SBC-sw 6.1.2025 880 W·m^{-2}	195	0.0177	8100	3.3	11.44	92.66	0.475
SBC-sw 11.1.2025 885 W·m^{-2}	188	0.0188	8100	3.3	11.72	94.92	0.505
13-20.1.2025	*Rain in village; snow on Mt. Psiloritis and Likia Ori*						
SBC-sw 1.2.2025 916 W·m^{-2}	184	0.0222	7140	3.3	13.49	96.34	0.52
4 - 12.2.2025	*Cloud and rain and in village; local snow down to* 1000 *m*						
SBC-sw 13.2.2025 940 W·m^{-2}	189	0.0222	8100	3.3	13.86	112.27	0.59
18-24.2.2025	*HNMS cold front "Coral" warning, local snow down to* 900 *m*						
SBC-sw 26.2.2025 960 W·m^{-2}	184	0.2055	8100	3.3	12.48	102.09	0.54
SBC-sw Mean value	178.5	0.0203	7914	3.3	12.07	94.82	0.53

Now consider that the data within **Table 5** represents measurements staring at 11 a.m. with an approximation two-hour duration, calendar date, and fixed geographical location on the Earth's spherical surface. Using this premise, a 2-dimensional plot of imparted egg energy density (vertical axis) as a function solar irradiance (horizontal axis) provides energy phase-space information on the solar cooking process **Figure 7**. In this projection the solar irradiance axis has a linear scale that allows a simple linear regression analyses. Even so when the axis is transformed into clock-time (measured in days) more complex information is revealed. For example, the fixed SBC-s data points (black filled circles), and the SBC-sw data points (open circles and open squares) can be placed in context of the winter solstice, and the vernal equinox that marks the beginning spring.

For the linear regression on the ten data points, Microsoft Excel linear regression yields a linear model ($y = mx + b$, where $m = 0.0007$, and $b = -0.0801$) over solar irradiance range of 873 to 1004 W·m^{-2}, and energy density of 0.463 to 0.58 kJ·g^{-1}. This model is represented by the black trend-line that has a mid-range goodness of fit (R^2) value of 0.4722 that indicates that 47.22 % of the data variance is attributed to the model. In practice though the intercept value should represent no sunlight, or zero on the y axis. Given these physical criteria the model becomes

$y = 0.0006$, with $R^2 = 0.4641$. From this knowledge, both models are descriptive with experimental factors influencing the data point values. The following factors may be considered:

1) The energy data are normalized to egg mass (power multiplied by time then divided by egg mass ($kJ \cdot g^{-1}$)) thus when the SBC inclined widow is adjusted for winter and summer seasons differential information between the two SBC-types is removed.

2) The mathematical analysis takes into account variations in daily ambient temperature as power is computed using Equations (4), where ΔT is the change in temperature of the heated eggs-without water (final temperature minus the initial temperature).

3) A likely source of the data variance is that the Sun's altitude angle increases with the solar cooking time, and energy transfer efficiency through the double-glazed window increases as solar noon approaches.

4) A further likely source of data variance is that the SBC alignment to the Sun is performed manually every 15 to 20 minutes.

5) The eggs-without-water cooking time is a coarse estimation using a time-stamp interval of five minutes.

6) Clear sky days are selected for the solar cooking study. However, the presence of fin high cloud cover and changes in relative humidity may also contribute to the data variance.

With this combination of factors it is reasonable to assume that they contribute to the uncounted 52.78% (100 minus 47.22%) data variance. Nevertheless the model indicates that the solar irradiance can be used to predict total egg mass

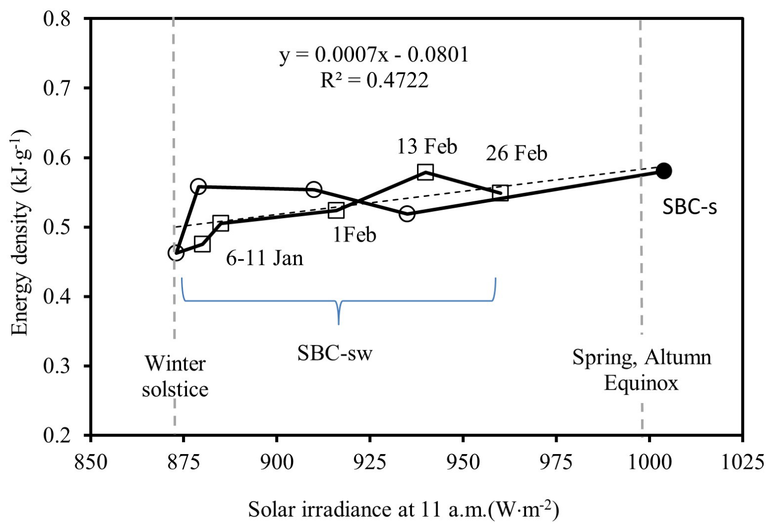

Figure 7. Solar cooking of fresh whole eggs-without water: data taken from **Table 5**. Black filled circle represents the SBW-s on 7.7.2024. Open-filled circles represent SBC-sw measurements between November and December 2024. Open squares represent SBC-sw measurements between January and February 2025. Dashed trend-line is the linear regression, and the thick solid line depicts the sequence of measurements.

cooking time, where the preference in boiled egg texture is adjusted by increasing or decreasing the model trend-line slope while keeping the intercept equal to zero. This predictive value needs further investigation with a focus on the model being "scale free" with regard to SBC-type.

Using the same premise as above, the timestamp of each data point can be linked consecutively producing an apparent figure of 8 (black solid-line within Figure 7) that suggests an Earth's analemma (J Lynch (2012) [35], and Jenkins (2013) [36]) is operating, where the SBC acts as a convoluted sun dial. However, at the 26th February data point where the second loop begins to close the full year is not complete. From this knowledge, the erroneous analemma assumption gives weight to the initial, and simple, observation of a strong data variance within the linear regression model.

6. Summary

This work has presented a winterized SBC for solar cooking on at a location (35.31˚N, 24.31˚E, altitude of 150 m) on the island of Crete located in the Eastern Mediterranean sea. The SBC requires winterization to match the Sun's seasonal low altitude angle, and protection from prolonged heavy rain periods and strong winds. For two months on either side of the winter solstice, a systematic solar cooking study is undertaken. The foodstuff of choice is fresh whole eggs and solar cooked without water. In this period consecutive rain and storm systems reduce solar cooking days in January to 10 to 14 days, and February to 4 to 8 days.

During this four-month winter period analysis of the cooking data reveals that the SBC-sw energy required to cook eggs-without water is 0.53 ± 0.06 kJ·g^{-1}. This value compares favourably (0.58 kJ·g^{-1}) for the SBC-s at the same location in the month of July 2024 thereby fulfilling the first aim of this study. To obtain this goal the SBC-sw was stored indoors for the months of December, January and February and only out on the sunshine days selected for solar cooking. Under these conditions pre-heating of SBC was the same as for the SBC-s. Thus the second aim was obtained by employing a simple protective storage solution.

Given the knowledge that storms can cut-off rural communities from the centralised electrical supply, contaminate water supplies, inundate firewood, and prevent the resupply of cooking fuel due to damaged road infrastructure. During this short emergency period, people still need access to cooked food. This work demonstrates the proof of principle that the inclusion of a winterized SBC into a family emergency/disaster preparedness plan enables the family to supplement their limited cooking fuel stock with solar cooking in sunshine hours.

Conflicts of Interest

The authors declare that they have no conflicts of interest.

References

[1] Kerr, B.P. (1991) The Expanding World of Solar Box Cookers. Publisher Barbara P

Kerr.

[2] Regattieri, A., Piana, F., Bortolini, M., Gamberi, M. and Ferrari, E. (2016) Innovative Portable Solar Cooker Using the Packaging Waste of Humanitarian Supplies. *Renewable and Sustainable Energy Reviews*, **57**, 319-326. https://doi.org/10.1016/j.rser.2015.12.199

[3] Law, V.J., Lalor, J.F. and Dowling, D.P. (2024) Inclined Window Solar Box Cooker with One External Reflector Designed for the Mediterranean Latitudes. Journal *of Power and Energy Engineering*, **12**, 1-33. https://doi.org/10.4236/jpee.2024.1211001

[4] Qandil, A., Al-Younis, E.S., Saleh, A. and Hasson, M. (2018) Experimental Study of the Performance of a Box Solar Cooker. *International Journal of Scientific & Engineering Research*, 9, 769-773.

[5] Benbaha, A., Yettou, F., Azoui, B., Gama, A., Rathore, N. and Panwar, N.L. (2024) Novel Mixed Solar Cooker: Experimental, Energy, Exergy, and Economic Analysis. *Heat Transfer*, **53**, 2095-2127. https://doi.org/10.1002/htj.23023

[6] Maammeur, H., Rouag, A., Belatrache, D., Bendaoud, B. and Moussaoui, Y. (2024) Experimental Investigation on Two Novel Standard Parameters to Improve the Performance of Solar Box Cookers. *Annals of West University of Timisoara-Physics*, **66**, 95-117. https://doi.org/10.2478/awutp-2024-0007

[7] Belatrache, D., Necib, H., Maammeur, H., Chaich, Z., Bougoffa, E. and Djeghab, A. (2024) Experimental Study of the Influence of Wing Reflectors on Solar Hot Box Cooker Performance. *International Journal of Environmental Science and Technology*, **22**, 4481-4494. https://doi.org/10.1007/s13762-024-05911-2

[8] Darhmaoui, H. and Lahjouji, D. (2013) Latitude Based Model for Tilt Angle Optimization for Solar Collectors in the Mediterranean Region. *Energy Procedia*, **42**, 426-435. https://doi.org/10.1016/j.egypro.2013.11.043

[9] Kambezidis, H.D. and Psiloglou, B.E. (2021) Estimation of the Optimum Energy Received by Solar Energy Flat-Plate Convertors in Greece Using Typical Meteorological Years. Part I: South-Oriented Tilt Angles. *Applied Sciences*, **11**, Article 1547.

[10] Abu-Naser, M. (2024) Tilt Angle Optimality Criteria for Stand Alone PV Systems. *Journal of Power and Energy Engineering*, **12**, 1-18. https://doi.org/10.4236/jpee.2024.123001

[11] Jaramillo, O.A., Huelsz, G., Hernández-Luna, G., del Río, J.A., Acosta, R. and Arriaga, L.G. (2007) Solar Oven for Intertropical Zones: Optogeometrical Design. *Energy Conversion and Management*, **48**, 2649-2656. https://doi.org/10.1016/j.enconman.2007.04.021

[12] Chatelain, T., Mauree, D., Taylor, S., Bouvard, O., Fleury, J., Burnier, L., *et al.* (2019) Solar Cooking Potential in Switzerland: Nodal Modelling and Optimization. *Solar Energy*, **194**, 788-803. https://doi.org/10.1016/j.solener.2019.10.071

[13] Al-Nehari, H.A., Mohammed, M.A., Odhah, A.A., Al-attab, K.A., Mohammed, B.K., Al-Habari, A.M., *et al.* (2021) Experimental and Numerical Analysis of Tiltable Box-Type Solar Cooker with Tracking Mechanism. *Renewable Energy*, **180**, 954-965. https://doi.org/10.1016/j.renene.2021.08.125

[14] Greenberg, E., Price, C., Yair, Y., Ganot, M., Bór, J. and Sátori, G. (2007) ELF Transients Associated with Sprites and Elves in Eastern Mediterranean Winter Thunderstorms. *Journal of Atmospheric and Solar-Terrestrial Physics*, **69**, 1569-1586. https://doi.org/10.1016/j.jastp.2007.06.002

[15] Detring, C., Müller, A., Schielicke, L., Névir, P. and Rust, H.W. (2021) Occurrence and Transition Probabilities of Omega and High-over-Low Blocking in the Euro-Atlantic Region. *Weather and Climate Dynamics*, **2**, 927-952.

https://doi.org/10.5194/wcd-2-927-2021

[16] Lagouvardos, K., Dafis, S., Giannaros, C., Karagiannidis, A. and Kotroni, V. (2020) Investigating the Role of Extreme Synoptic Patterns and Complex Topography during Two Heavy Rainfall Events in Crete in February 2019. *Climate*, **8**, Article 87.

[17] Soro, D., Soro, D., Sidibé, M., Doumbia, Y., Touré, S. and Marí, B. (2020) Theoretical and Experimental Studies of a Box-Type Solar Cooker in Unfavorable Climatic Conditions. *Smart Grid and Renewable Energy*, **11**, 51-60. https://doi.org/10.4236/sgre.2020.114004

[18] (2025) Solar Cooker International. https://solarcookers.org/

[19] https://www.solarcooker-at-cantinawest.com/

[20] Ciochetti, D.A. and Metcalf, R.H. (1984) Pasteurization of Naturally Contaminated Water with Solar Energy. *Applied and Environmental Microbiology*, **47**, 223-228. https://doi.org/10.1128/aem.47.2.223-228.1984

[21] Cooking Eggs Sous Vide. https://www.scienceofcooking.com/eggs/cooking-eggs-sous-vide.html

[22] https://www.youtube.com/watch?v=1cE0geJY1SI

[23] Terres, H., Lizardi, A., López, R., Vaca, M. and Chávez, S. (2014) Mathematical Model to Study Solar Cookers Box-Type with Internal Reflectors. *Energy Procedia*, **57**, 1583-1592. https://doi.org/10.1016/j.egypro.2014.10.150

[24] Arabacigil, B., Yuksel, N. and Avci, A. (2015) The Use of Paraffin Wax in a New Solar Cooker with Inner and Outer Reflectors. *Thermal Science*, **19**, 1663-1671. https://doi.org/10.2298/tsci121022031a

[25] Bhaumik, M., Sur, A. and Pasi, B. (2018) Design and Development of Economic and Portable Solar Cooker System Using Waste Materials. *Journal of Basic and Applied Research International*, **24**, 104-112.

[26] Cuce, P.M., Kolayli, S. and Cuce, E. (2020) Enhanced Performance Figures of Solar Cookers through Latent Heat Storage and Low-Cost Booster Reflectors. *International Journal of Low-Carbon Technologies*, **15**, 427-433. https://doi.org/10.1093/ijlct/ctz079

[27] Kumar, A., Saxena, A., Pandey, S.D. and Joshi, S.K. (2022) Design and Performance Characteristics of a Solar Box Cooker with Phase Change Material: A Feasibility Study for Uttarakhand Region, India. *Applied Thermal Engineering*, **208**, Article 118196. https://doi.org/10.1016/j.applthermaleng.2022.118196

[28] Kumar, A., Saxena, A., Pandey, S.D. and Gupta, A. (2023) Cooking Performance Assessment of a Phase Change Material Integrated Hot Box Cooker. *Environmental Science and Pollution Research*, **31**, 62392-62407. https://doi.org/10.1007/s11356-023-25340-x

[29] Ibrahim, O.A.A., Kadhim, S.A. and Ali, H.M. (2024) Enhancement the Solar Box Cooker Performance Using Steel Fibers. *Heat Transfer*, **53**, 1660-1684. https://doi.org/10.1002/htj.23008

[30] Poonia, S. and A K Singh, (2024) Economic and Environmental Sustainability of Various Solar Thermal Devices. *Annals of Arid Zone*, **63**, 9-19. https://doi.org/10.56093/aaz.v63i2.147200

[31] Čekon, M., Struhala, K. and Slávik, R. (2017) Cardboard-Based Packaging Materials as Renewable Thermal Insulation of Buildings: Thermal and Life-Cycle Performance. *Journal of Renewable Materials*, **5**, 84-93. https://doi.org/10.7569/jrm.2017.634135

[32] Collares-Pereira, M., Cavaco, A. and Tavares, A. (2018) Figures of Merit and Their Relevance in the Context of a Standard Testing and Performance Comparison Meth-

ods for Solar Box—Cookers. *Solar Energy*, **166**, 21-27.
https://doi.org/10.1016/j.solener.2018.03.040

[33] Folaranmi, J. (2013) Performance Evaluation of a Double-Glazed Box-Type Solar Oven with Reflector. *Journal of Renewable Energy*, **2013**, Article 184352.
https://doi.org/10.1155/2013/184352

[34] Coimbra, J.S.R., Gabas, A.L., Minim, L.A., Garcia Rojas, E.E., Telis, V.R.N. and Telis-Romero, J. (2006) Density, Heat Capacity and Thermal Conductivity of Liquid Egg Products. *Journal of Food Engineering*, **74**, 186-190.
https://doi.org/10.1016/j.jfoodeng.2005.01.043

[35] Lynch, P. (2012) The Equation of Time and the Analemma. *Irish Mathematical Society Bulletin*, **69**, 47-56. https://doi.org/10.33232/bims.0069.47.56

[36] Jenkins, A. (2013) The Sun's Position in the Sky. *European Journal of Physics*, **34**, 633-652. https://doi.org/10.1088/0143-0807/34/3/633